Available online at www.sciencedirect.com
ScienceDirect
Journal of Power Sources 174 (2007) 1057–1062
JOURNAL OF POWER SOURCES
www.elsevier.com/locate/jpowsour

Short communication

Preparation of lithium manganese oxide fine particles by spray pyrolysis and their electrochemical properties

Y. Iriyama [a,*], Y. Tachibana [b], R. Sasasoka [a], N. Kuwata [c], T. Abe [a], M. Inaba [b], A. Tasaka [b], K. Kikuchi [d], J. Kawamura [c], Z. Ogumi [a]

[a] *Department of Energy and Hydrocarbon Chemistry, Graduate School of Engineering, Kyoto University, Nishikyo-ku, Kyoto 615-8510, Japan*
[b] *Department of Molecular Science and Technology, Faculty of Engineering, Doshisha University, Kyotanabe, Kyoto 610-0321, Japan*
[c] *Institute for Multidisciplinary Research of Advanced Materials, Tohoku University, Katahira 2-1-1, Aobaku, Sendai 980-8577, Japan*
[d] *Department of Materials Science, The University of Shiga Prefecture, Hikone, Shiga 552-8533, Japan*

Available online 30 June 2007

Abstract

Highly crystalline nano-sized lithium manganese oxide particles were fabricated by spray pyrolysis. The resultant particles had well-developed facet planes in a transmission electron microscopy (TEM) image and electron diffraction pattern from a single particle also showed clear diffraction spots, indicating that the prepared particles were highly crystalline. The mean crystallite size estimated from X-ray diffraction peaks was ca. 18 nm, which was in good agreement with the diameter of the particles observed in the TEM image. These particles were gathered on platinum mesh and their electrochemical properties were investigated. The mean crystallite size increased with an increase in annealing temperature, which influenced the electrochemical lithium insertion/extraction properties of the particles. In particular, samples annealed at 773 K showed different kinds of lithium extraction/insertion properties in the cyclic voltammogram (CV), and only a couple of broad redox peaks were observed at around 0.8 V (versus Ag/AgCl) between 0.4 and 1.0 V. It is suggested that lithium distribute randomly in the sample annealed at 773 K sample due to the effects of grain boundaries, which resulted in different kinds of phase transition reactions.

Keywords: Rechargeable lithium batteries; Fine particles; Lithium manganese oxide; Phase transition

1. Introduction

Rechargeable lithium batteries have been widely used as a power source for portable devices because of their high energy density. In recent years, this battery system has received much attention as a power source for large-sized devices such as electric and hybrid vehicles, satellites, and trains. These demands have motivated the development of advanced rechargeable lithium batteries with higher energy and power density, lower cost, longer life, and improved safety.

The use of fine particles as electrode active materials is expected to decrease the lithium diffusion length in the active material and to increase its specific surface area effectively. These advantages will result in a reduction of cell resistance due to diffusion of lithium in the active material and charge transfer reaction, leading to the increase of power density of rechargeable lithium batteries. In addition, nano-sized fine particles have possibilities to provide other useful functions as published by many interesting reports [1–4]. Thus, the use of fine particles as electrode active materials must be one of the key technologies in developing advanced rechargeable lithium batteries. Nano-sized electrode active particles have high specific surface area and then they tend to aggregate easily each other to decrease their surface energy in general. The grain boundaries provided by aggregation of nano-sized electrode active materials will dominate relatively large volumes in the aggregated particle. Hence, the effects of the grain boundaries on the electrochemical lithium insertion/extraction properties should be investigated to allow the design of rechargeable lithium batteries with higher performances.

Nano-sized particles have been successfully prepared by various methods, such as the spray pyrolysis method [5,6], sol–gel method [7,8], and hydrothermal method [9–11]. Of these, this work focused on the spray pyrolysis method because the particles can be fabricated in gas phase and then they can be easily collected on a substrate (current collector) without any

* Corresponding author. Tel.: +81 75 383 2485; fax: +81 75 383 2488.
E-mail address: iriyama@elech.kuic.kyoto-u.ac.jp (Y. Iriyama).

0378-7753/$ – see front matter © 2007 Elsevier B.V. All rights reserved.
doi:10.1016/j.jpowsour.2007.06.193

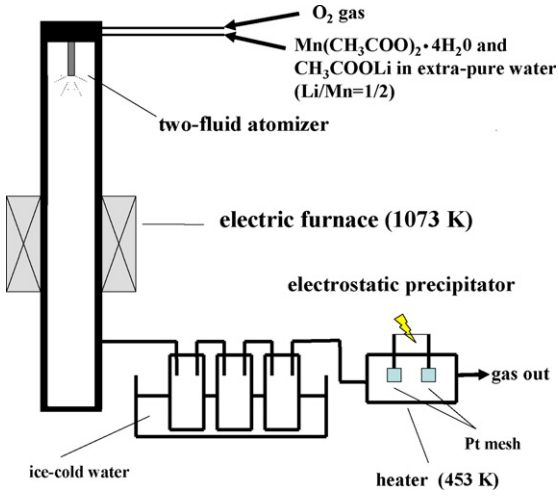

Fig. 1. Schematic image for spray pyrolysis apparatus.

impurities such as conductive additives and binder. Moreover, it is generally recognized that the size distribution fabricated by spray pyrolysis is narrow and the purity of the products is high [5]. These are important advantages for investigating electrochemical properties of the resultant electrode active materials themselves. In this work, lithium manganese oxide fine particles were prepared by spray pyrolysis and the effects of grain boundaries of nano-particles on their electrochemical properties were investigated.

2. Experimental

Fine particles of lithium manganese oxide were prepared using the spray pyrolysis apparatus shown in Fig. 1, and the preparation conditions are summarized in Table 1. Both $Mn(CH_3COO)_2 \cdot 4H_2O$ and CH_3COOLi were dissolved in extra-pure water. The Li/Mn ratio in the solution was 0.50, which was used as the starting solution. The lithium concentration in the solution was either 0.01 or 0.02 mol dm^{-3}. A two-fluid atomizer was attached at the top of the apparatus, where both oxygen gas and the starting solution was flowed top-to-bottom into the quartz reaction tube. The furnace was set in the bottom side of the quartz tube and was heated to 1073 K during the preparation. Prepared particles for electrochemical measurements were passed through three traps cooled by ice-cold water and collected on platinum 100 mesh by electrostatic precipitator heated at 453 K. The pulsed voltage of 3 kV was applied for the precipitation. The resultant particles deposited on the platinum mesh were annealed at 773 or 973 K for 2 h in air. Some of the particles were specially gathered in water after filtering by differential mobility analyzer to observe particle shape precisely by TEM observation.

Table 1
Summary of preparation conditions of lithium manganese oxide fine particles

Electric furnace temperature	1073 K
Composition of starting solution	Li:Mn = 1:2
Gas flow rate	14 l min^{-1} (O_2)
Liquid flow rate	5 ml min^{-1}
Applied pulsed voltage for electric precipitator	3 kV
Temperature during the gathering	423 K

The resultant particles deposited on the platinum mesh were characterized by X-ray diffraction spectroscopy (Rigaku RINT 2500), transmission electron microscopy (HITACHI H-9000NAR), and ^{7}Li MAS NMR. The ^{7}Li MAS NMR measurements were performed at 155.6 mHz on a Bruker AVANCE 400 spectrometer with a 2.5 mm MAS probe spinning at 35 kHz. The resultant NMR spectra were recorded using a rotor synchronized spin-echo experiments. All spectra were referenced to 1 mol dm^{-3} LiCl solution at 0 ppm. A $\pi/2$ pulse of 1.5 μs was used with a delay time of 0.3 s. The particles gathered in water after filtering were also characterized by electron diffraction. The Li/Mn ratio of the particles was measured by inductively coupled plasma spectroscopy (PerkinElmer OPTIMA 4300DV).

Electrochemical properties of the resultant samples were measured using three electrodes cell. Because of the high reactivity of the fine particles with conventional organic liquid electrolyte, aqueous solution was used as the liquid electrolyte to investigate the electrochemical properties of the samples. The working electrode was platinum mesh with the particles. The reference electrode was Ag/AgCl saturated by NaCl (BAS RE-1B), and the counter electrode was platinized platinum wire. The electrolyte was 1 mol dm^{-3} $LiCF_3SO_3$ dissolved in extra-pure water. Electrochemical properties of the samples were measured by cyclic voltammetry and AC impedance spectroscopy at room temperature.

3. Results and discussion

Fig. 2 shows a TEM image of the filtered particles prepared from the 0.02 mol dm^{-3} solution. The particles had polygon structures and facet planes appeared clearly. A typical electron diffraction pattern measured from one of these particles is shown in the inset in Fig. 1 and clear diffraction spots were observed. These results indicate that the as-prepared particles were highly crystalline.

Fig. 3 shows TEM images of the samples deposited on platinum mesh with and without annealing. All these samples were prepared from the 0.01 ml dm^{-3} solution. In the as-prepared sample, uniform-sized particles with 10–20 nm in

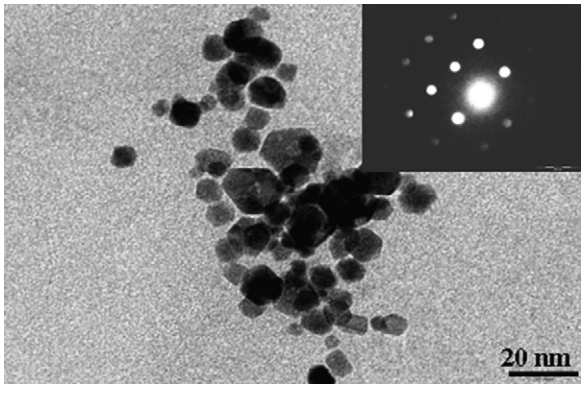

Fig. 2. TEM image of lithium manganese oxide fine particles. The inset shows the electron diffraction pattern from single crystal in the image.

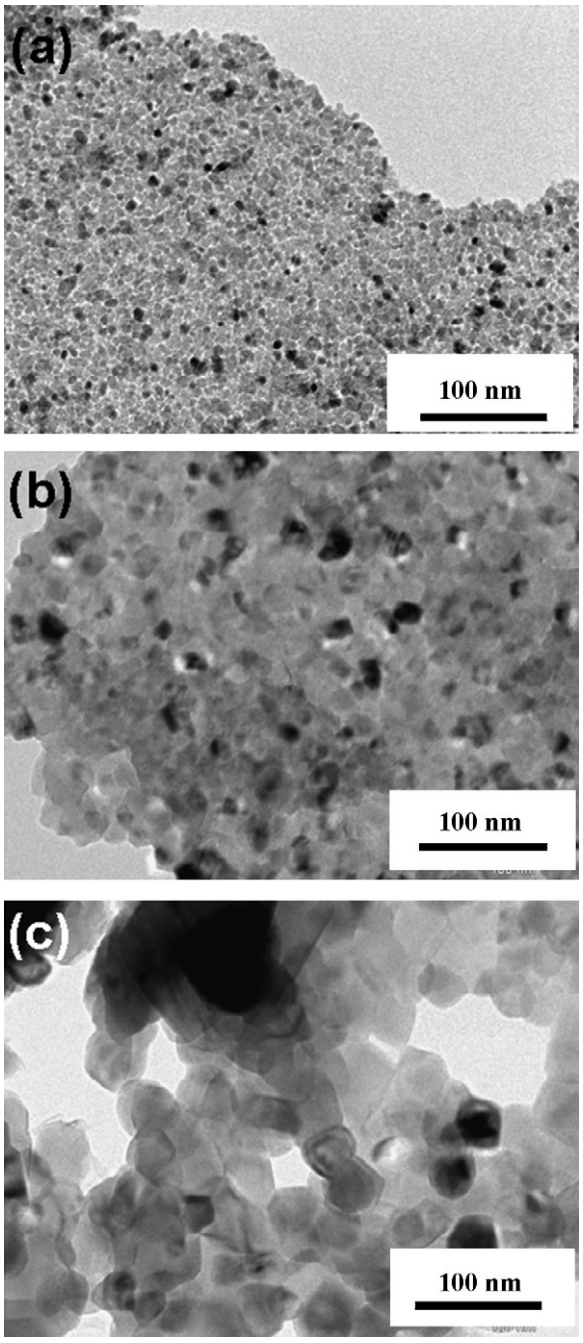

Fig. 3. TEM image of lithium manganese oxide fine particles of (a) as-prepared, (b) 773 K-annealed, and (c) 973 K-annealed samples.

diameter aggregated each other. The geometric structure of particles resembled to that of Fig. 2 and their grain boundaries were visibly observed as shown in Fig. 3a. When the as-prepared sample was annealed at 773 K, the particles aggregated densely and their grain boundaries were not clearly observed (Fig. 3b). After the sample was annealed at higher temperature, 973 K, the particles grew over 50 nm as shown in Fig. 3c. Hereafter, particles deposited on platinum mesh with annealing at 773 and 973 K are referred to as 773 K- and 973 K-samples, respectively. Inductively coupled plasma spectroscopy measurements revealed that the Li/Mn ratio in the as-prepared sample was 0.51.

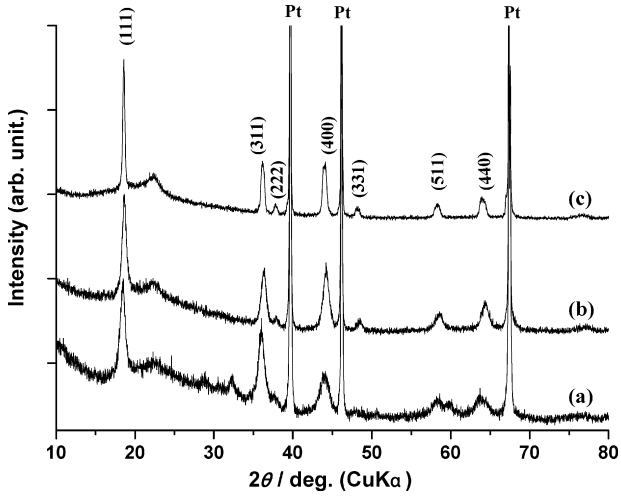

Fig. 4. XRD patterns of lithium manganese fine particles deposited on platinum mesh of (a) as-prepared, (b) 773 K-annealed, and (c) 973 K-annealed particles.

X-ray diffraction patterns of these samples are summarized in Fig. 4. Peak position of these data was normalized by diffraction peaks of Pt (1 1 1). A broad diffraction peak at around 22° was from both glass plate and adhesive tape used for mounting the sample on the X-ray measurement holder. Diffraction peaks assigned to spinel-structured lithium manganese oxide were observed in all samples [12]. The full width at half maximum (FWHM) of diffraction peaks varied by the annealing. The average crystallite size of these samples was estimated using conventional Scherrer equation, which are summarized in Table 2. The average crystallite size of the as-prepared sample were calculated to be ca. 18 nm, which was in reasonable agreement with the mean particle diameter estimated by TEM image shown in Fig. 3a. The average crystallite size did not largely increase by annealing at 773 K (ca. 22 nm), but it increased to ca. 74 nm by annealing at 973 K. The larger particle size formed by the 973 K annealing is also consistent with the TEM image shown in Fig. 3c. In the 773 K-sample, particles appear to interact strongly with each other in TEM image, but XRD analysis revealed that the average crystallite size remained similar to that in the as-prepared condition, indicating that the spinel host structure did not grow much by the 773 K annealing.

Fig. 5 shows the ^{7}Li MAS NMR spectra of the as-prepared and 773 K-samples. The NMR spectrum of spinel-structured $LiMn_2O_4$ particle prepared by conventional solid-state reaction was also measured using the same conditions as a reference spectrum, where sharp isotropic ^{7}Li resonance assigned to Li occupation at 8a site in $LiMn_2O_4$ is mainly observed around 500 ppm [13]. The isotropic resonance of the as-prepared sam-

Table 2
Average crystallite size of lithium manganese oxide fine particles calculated from the Scherrer equation using diffraction peak from (1 1 1) planes in Fig. 4

	Average crystallite size (nm)
As-prepared	18.4
Annealed at 773 K	21.6
Annealed at 973 K	73.9

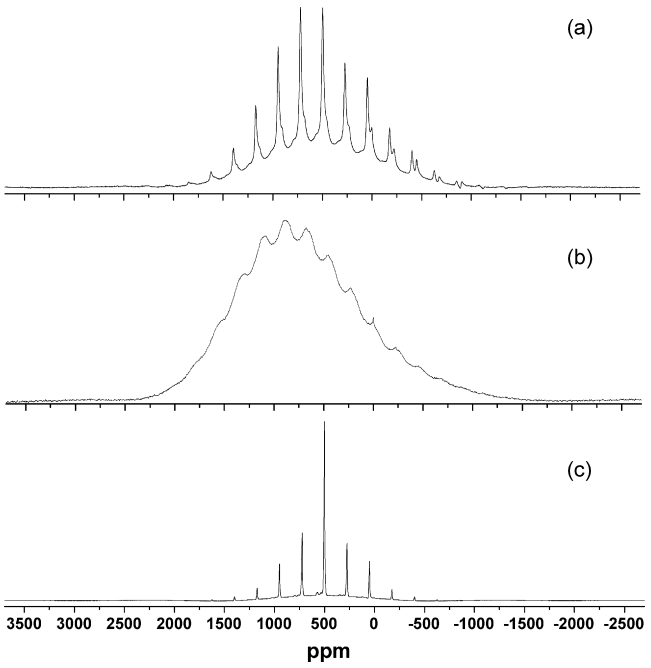

Fig. 5. ^{7}Li MAS NMR spectra of lithium manganese oxide fine particles gathered on platinum mesh of (a) as-prepared and (b) 773 K-annealed. (c) ^{7}Li MAS NMR spectrum of lithium manganese oxide prepared by conventional solid-state reaction at 973 K. This spectrum was observed by the same conditions with the above particles and is shown as reference spectrum.

ple was observed around 500 ppm and their spinning sidebands were also observed as with the case of the reference spectrum. An impurity isotropic resonance was also observed at close to 0 ppm, which may be due to some diamagnetic lithium-containing impurity formed in the sample or lithium near the fine particle surface. The 773 K-sample did not show these sharp resonances and broader isotropic resonance was alternatively observed centering around 900 ppm. Lee et al. investigated ^{6}Li MAS NMR spectra of various kinds of lithium manganese oxide samples. They showed that an increase of manganese oxidation state from (III) to (IV) results in a NMR peak shift to higher frequency and that ^{6}Li MAS NMR peak of such a Mn^{4+} phase becomes broader than that of $LiMn_2O_4$ [13]. Hence, it is suggested that the peak shift observed in the 773 K-sample originates from the presence of Mn^{4+}. Because XRD patterns did not show any remarkable changes and, as described later, the 773 K-sample showed lithium insertion/extraction reaction at the potential nearly consistent with $Li_xMn_2O_4$ ($0 < x < 1$) unlike that of Mn^{4+} compounds such as $Li_4Mn_5O_{12}$ [14] and Li_2MnO_3 [15], Mn^{4+} will be formed in part of the 773 K-sample. Hence, a broad resonance of the 773 K-sample will be ascribed to the presence of Mn^{4+}.

Fig. 6 shows the CVs of the samples in aqueous solution. The potential was swept at 1 mV s^{-1} between 0.4 and 1.0 V (versus Ag/AgCl). Both the 973 K- and as-prepared samples revealed two couples of redox peaks, which is typical of the electrochemical lithium insertion/extraction reaction of spinel-structured $LiMn_2O_4$ [16]. It is interesting to note that the 773 K-sample showed a totally different shape in its CV, and only a couple of broad redox reaction peak without minima was observed

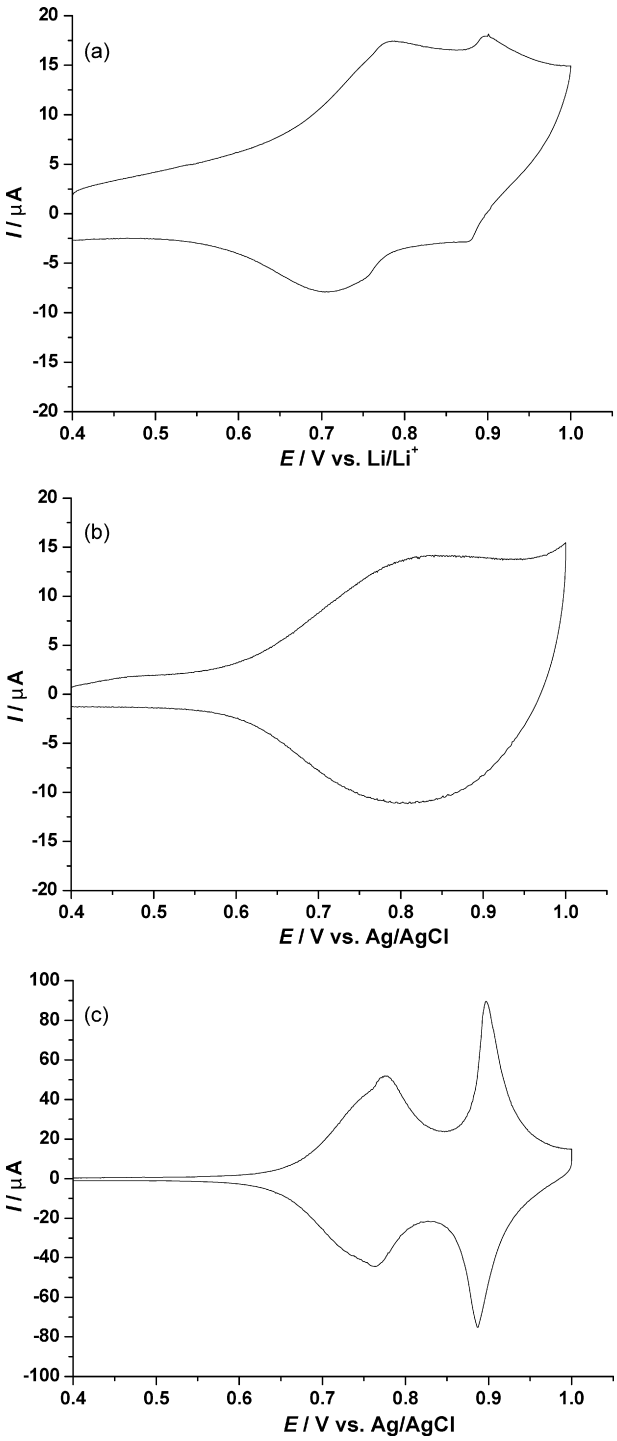

Fig. 6. Cyclic voltammogram of lithium manganese oxide fine particles deposited on platinum mesh in 1 mol dm^{-3} $LiCF_3SO_3$ dissolved in extra-pure water. (a) As-prepared, (b) 773 K-annealed, and (c) 973 K-annealed particles.

at around 0.8 V (versus Ag/AgCl). Most probable reason will be that lithium in the 773 K-sample is presented in disordered state. Such disordered state will produce a random variation in the lithium–lithium interaction in the host structure, resulting in broad redox peak like a single phase reaction [17]. Both the particle size and X-ray diffraction peaks of the 773 K-sample were nearly identical with the as-prepared sample, where

lithium located regularly in the host structure as for conventional $LiMn_2O_4$. Therefore, it will not be reasonable to expect that such disordered state of lithium in the 773 K-sample is an effect of particle size. The particles of the 773 K-sample appeared to coalesce strongly as shown in Fig. 3b, thus we speculate that the formation of Mn^{4+} in the 773 K-sample is mainly because easily mobile lithium segregate at grain boundaries during the grain growth of these particles with the formation of Mn^{4+} in the particle. At that case, concentration profile of lithium in the particle will be largely distorted, resulting in the disordered state of lithium in the particles. These properties are not observed in the CV of the 973 K-sample, which is probably because the particles grew so large that such grain boundary effects would not affect the total reaction.

The redox peak separation at the lower potential of the as-prepared sample in CV was 71 mV, which was much larger than that of the 973 K-sample (12 mV). AC impedance measurement was conducted for the as-prepared sample at 0.76 V (versus Ag/AgCl). The Cole–Cole plot shown by closed circles in Fig. 7 was consisted of semicircular arc at the high frequency region, which is assigned to charge transfer reaction, followed by a straight line with a slope of 45°, which corresponds to semi-infinite diffusion. This diffusion reaction was not saturated even at 100 mHz. Cole–Cole plot of highly crystalline $LiMn_2O_4$ thin film electrode with 60 nm in thickness [15] was also shown in Fig. 7 for comparison; it consists of a semicircular arc assigned to charge transfer reaction and straight line vertical to the real axis assigned to infinite diffusion. The thickness of the film electrode was larger than that of the average particle size of the as-prepared particles, but semi-infinite property was not observed at all. This indicates that lithium diffusion in the as-prepared electrode material is largely retarded, resulting in larger peaks separation in the CV. Lower diffusivity of lithium itself in small-sized particles has been pointed out for lithium insertion/extraction reactions of $Li_{4/3}Ti_{5/3}O_4$ and $LiCoO_2$ [4,18]. However, reactivity of those fine particles will be strongly influenced also by the crystallinity of the particles. In fact, in case of lithium insertion reaction into nano-sized highly crystalline α-MoO_3, in-plane lithium transport proceeded quite fast [19]. The crystallinity of the as-prepared particles is very high and then it is speculated that lithium diffusion in the as prepared highly crystalline particles would proceed rapidly also in case of lithium manganese oxide. On the other hand, difficulty of ion transport across the grain boundaries have been shown visually in case of lithium ion transport into graphite [20] and of oxygen ion transport into $SrTiO_3$ [21]. From the above consideration, we believe at present that this largely retarded diffusivity of lithium originates from the difficulty of lithium transport across grain boundaries.

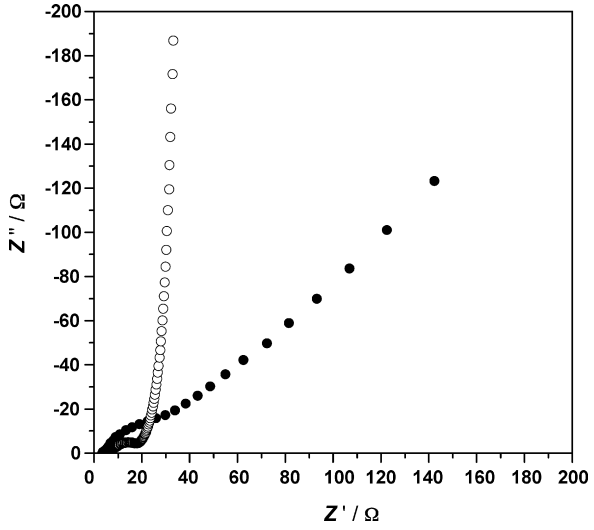

Fig. 7. Cole–Cole plots of highly crsytalline $LiMn_2O_4$ thin film deposited on platinum mech (◯) and the fine particle of lithium manganese oxide deposited on platinum mesh (●). Both spectra were measured at 0.76 V in aqueous solution (1 mol dm^{-3} $LiCF_3SO_3$ dissolved in extra-pure water) at room temperature.

Even though nano-sized particles showed high crystallinity, grain boundaries of them were formed easily. These grain boundaries appear to affect both phase transition mechanism and the kinetics of electrochemical lithium insertion/extraction properties of lithium manganese oxide. These results strongly suggest that regulation of the grain boundaries between the particles must play an important role in the design of advanced lithium-ion batteries using nano-sized electrode active materials in the practical application.

4. Conclusions

Nano-sized lithium manganese oxide particles (Li/Mn = 0.51) were prepared by spray pyrolysis. The as-prepared particles were of uniform size with ca. 18 nm in diameter and their crystallinity was very high. These particles were gathered on platinum mesh and then annealed at different temperatures. Effects of grain boundaries of nano-particles on their electrochemical properties were mainly investigated. Although the detailed mechanisms have not been clarified in this work, these grain boundaries formed in nano-sized electrode active materials appear to affect both the phase transition mechanism and the kinetics of electrochemical lithium insertion/extraction properties of lithium manganese oxide. The sample annealed at 773 K showed different kinds of lithium extraction/insertion properties in the cyclic voltammogram (CV), and only a couple of broad redox peak was observed at around 0.8 V (versus Ag/AgCl) between 0.4 and 1.0 V. It is suggested that lithium distribute randomly in the 773 K-sample due to the effects of grain boundaries, which resulted in different kinds of phase transition reactions. Both the as-prepared and 973 K-annealed samples showed redox reaction peak in CV as with conventional spinel-structured $LiMn_2O_4$. However, redox peak potential of the as-prepared sample was separated largely because of lower diffusivity of lithium in the electrode. This lower diffusivity should be ascribed to the difficulty of the lithium diffusion across grain boundaries.

Acknowledgements

This work was supported by the Ministry of Education, Science, Sports and Culture, Grant-in-Aid for Scientific Research on Priority Areas, 439, 2004. This work was partially supported by New Energy and Industrial Technology Development Orga-

nization (NEDO) of Japan, and also by a Grant-in-Aid for 21st COE program-COE for a United Approach to New Materials Science from the Ministry of Education, Culture, Sports, Science, and Technology.

References

[1] J. Jamnik, J. Maier, Phys. Chem. Chem. Phys. 5 (2003) 5215.
[2] J. Jirkovskỳ, M. Makarova, P. Krtil, J. Electrochem. Soc. 152 (2005) 1613.
[3] J. Yamaki, M. Makidera, T. Kawamura, M. Egashira, S. Okada, J. Power Sources 153 (2006) 245.
[4] L. Kavan, J. Procházka, T.M. Spitler, M. Kalbáč, M. Zukalová, M. Grätzel, J. Electrochem. Soc. 150 (2003) A1000.
[5] I. Taniguchi, K. Matsuda, H. Furubayashi, S. Nakajima, AIChE J. 52 (7) (2006) 2413.
[6] S.H. Park, C.S. Yoon, S.G. Kang, H.-S. Kim, S.-I. Moon, Y.-K. Sun, Electrochim. Acta 49 (2004) 557.
[7] C. Julien, S.S. Michael, S. Ziolkiewicz, Int. J. Inorg. Mater. 1 (1999) 1.
[8] L. Kavan, M. Grätzel, Electrochem. Solid-State Lett. 5 (2002) A39.
[9] C. Kim, M. Noh, M. Choi, J. Cho, B. Park, Chem. Mater. 17 (12) (2005) 3297.
[10] Y. Zhang, H. Wang, B. Wang, H. Yan, A. Ahniyaz, M. Yoshimura, Mater. Res. Bull. 37 (2002) 1411.
[11] T. Adschiri, Y. Hakuta, K. Kanamura, K. Arai, High Pressure Res. 20 (2001) 373.
[12] JCPDS No. 35-0782.
[13] Y.J. Lee, F. Wang, C.P. Grey, J. Am. Chem. Soc. 120 (48) (1998) 12601.
[14] J. Kim, A. Manthiram, J. Electrochem. Soc. 145 (1998) L53.
[15] A.D. Robertson, P.G. Bruce, Chem. Mater. 15 (2003) 1984.
[16] Z. Ogumi, N. Nakayama, T. Nozawa, Y. Iriyama, T. Abe, K. Kikuchi, Extended abstract of International Meeting of Lithium Batteries, Biarritz, Abstracts #351, 2006.
[17] W.R. McKinnon, R.R. Haering, in: R.E. White, J. O'M. Bockris, B.E. Conway (Eds.), Modern Aspects of Electrochemistry, vol. 15, Prenum, 1983, p. 235.
[18] Y.-M. Choi, S.-I. Pyun, Solid State Ionics 99 (1997) 173.
[19] Y. Iriyama, T. Abe, M. Inaba, Z. Ogumi, Solid State Ionics 135 (2000) 95.
[20] A. Funabiki, M. Inaba, T. Abe, Z. Ogumi, Carbon 37 (10) (1999) 1591.
[21] M. Leonhardt, J. Jamnik, J. Maier, Electrochem. Solid-State Lett. 2 (1999) 333.